Chapter 16
Nanocomposite Materials – Ferroelectric Nanoparticles Incorporated into Porous Matrix

E. Rysiakiewicz-Pasek, R. Poprawski, A. Ciżman, and A. Sieradzki

Abstract The aim of this work is to develop a technique of introducing selected ferroelectric materials (TGS, $NaNO_2$, $NaNO_3$, KNO_3, ADP and KDP) into porous glasses with various average pore dimensions. The major efforts have been focused on the investigations of the influence of the pore size on physical properties and phase transition of nanocrystals embedded into porous matrix with different methods. The ferroelectrics have been introduced into porous glasses from the melt and a water solution. The results of electrical (dielectric, pyroelectric) and thermal (dilatometric and calorimetric) measurements have shown that the observed sequences of phase transitions in ferroelectric materials embedded into the porous glasses are similar to that in bulk crystals. The relationship between phase transition and melt temperatures versus average values of pore dimensions has been determined. The experimentally observed shift of phase transition temperatures is the superposition of the size effect and pressure effect created by the difference of thermal expansion coefficients of ferroelectrics nanoparticles and glass matrix.

Keywords Porous glasses • Nano-ferroelectrics • Phase transition

16.1 Introduction

Materials science world has become a very interesting research branch these days due to the creation of new materials with the development of new technologies to form them. A new material structure is designed to achieve as small sizes as

E. Rysiakiewicz-Pasek (✉) • R. Poprawski • A. Ciżman • A. Sieradzki
Institute of Physics, Wrocław University of Technology, Wyspiańskiego 27,
50-370 Wrocław, Poland
e-mail: ewa.rysiakiewicz-pasek@pwr.wroc.pl

Y.N. Shunin and A.E. Kiv (eds.), *Nanodevices and Nanomaterials for Ecological Security*, NATO Science for Peace and Security Series B: Physics and Biophysics, DOI 10.1007/978-94-007-4119-5_16,

possible and this becomes a priority of nanotechnology. The significance of nanotechnology-based material engineering has risen very much in recent years because in the nanometric scale the materials exhibit new interesting physical properties. The main goal of today is to create modern functional and structural materials with extraordinary properties by means of controlling materials composition and technological processes.

Ferroelectrics as the nonlinear materials show a series of physical properties which are extremely interesting in practical applications and scientific research. Dielectric, piezoelectric, pyroelectric and optical properties of ferroelectric materials are used to form non-volatile ferroelectric memories [1], micro-manipulators and nano-actuators used in AFM and STM, pyroelectric IR detectors, in light beam controllers and photonic crystals.

The introduction of ferroelectrics into the porous glass matrix with various pore sizes is one of the simplest ways of formation nanometric ferroelectrics. The investigation of the porous glasses filled with ferroelectric materials makes it possible to determine the dependence of the phase transition temperature and physical properties (electrical, thermal etc.) upon the crystal sizes. Most of available data on the porous glass based ferroelectric composites have been achieved from structural and dielectric studies and they have concerned $NaNO_2$ built into the pores. The phase transition temperature for $NaNO_2$ embedded into the glass pores was shifted towards lower temperatures when compared to that for the bulk crystal [2, 3]. Beside numerous works on studies of $NaNO_2$ in glass pores only few articles appear on studies of ferroelectrics built in the pores ($NaNO_3$, the Rochelle salt, TGS) [4, 5].

Our work concerns the art and technology of introducing TGS, $NaNO_2$, $NaNO_3$, KNO_3 and KDP-type crystals into porous glass (with various pore sizes) and the determining the phase transition temperature for these nano-ferroelectrics.

16.2 Sample Preparation and Investigation Methods

Silica porous glasses were obtained from the two-phase sodium-borosilicate glass by the method described in detail in [6]. Phase separation was enhanced by thermal treatments at 763 K (165 h) and 933 K (100 h). The borate phase was extracted by soaking the samples in hydrochloric acid. To remove silica gel present in the pores additional treatment in KOH was performed. Two types of porous glasses were fabricated: PG23 with average pore radius 23 nm (heated at 763 K) and PG 160 with 160 nm pores (heated at 933 K). The porosity determined from the mass decrement after etching was: 50% and 48% for PG23 and PG160, respectively. According to adsorption poroscopy and mercury porosimetry data, the total average pore volume was 364 mm^3/g for glass PG23 and 470 mm^3/g for glass PG160, the average surface area was 28.9 and 5.9 m^2/g for the respective samples.

KNO_3, $NaNO_2$, $NaNO_3$ was introduced into porous glass both from the melt and from a water solution. The glass plates were put into the melted salt (KNO_3 at

623 K, $NaNO_2$ at 578 K and $NaNO_3$ at 549 K). After 16 h the samples were taken out from the melt. The surfaces of glass were polished mechanically to remove small crystals.

In the second method the glass samples were immersed in a saturated water solution of $NaNO_2$, KNO_3, TGS, ADP and KDP at 353 K for 9 h. Then the samples were heated at 393 K for 1 h to remove the absorbed water. The process was repeated three times.

Dielectric measurements were performed by the Novocontrol Alpha impedance analyzer in the frequencies range from 0.1 Hz to 1 MHz.

Calorimetric investigations were performed using the differential scanning calorimeter (DSC) METTLER TOLEDO. The dielectric and calorimetric measurements were carried out on heating and on cooling at a constant temperature rate of 1 K/min.

Before pyroelectric measurements were performed, the samples had been polarized by an external electric field of the intensity of 4×10^5 V/m for 12 h at room temperature. Pyroelectric current was measured during the heating process with the rate of 1 K/min.

Dilatometric measurements were carried out with the precise self-made quartz capacitance dilatometer. The samples were heated to the desired high temperature and then cooled down at the rate of approximately 0.2 K/min.

All samples were heated at 363 K prior to the measurements to remove the residual water.

16.3 Physical Properties of Ferroelectrics Confined in Porous Glasses

Electron microscopic pictures of the fracture surface showed that all the investigated ferroelectrics filled well the glass pores [7]. The images obtained by the confocal microscopy (Fig. 16.1) for KNO_3 embedded into PG160 from the melt confirm the fullness of pores. The filling of pores for all nanonocomposites was estimated by the weight and it was equal to 80–90%. The elemental analysis of the results confirmed ferroelectric material presence in pores.

Porous glass embedded with TGS was the first nanomaterial under investigation. In Fig. 16.2 the dependence of the pyroelectric current on the temperature for glass PG23 and PG160 filled by TGS is shown. Bulk TGS single crystals exhibit the second-order ferroelectric phase transition at about 322 K from the $P2_1$ to $P2_1/m$ space group of the monoclinic system.

The existence of a jump of the pyroelectric current at the phase transition region indicates that TGS embedded into porous matrices exhibits ferroelectric properties. The phase transition temperature in composite porous glasses-TGS is higher than that for bulk TGS crystals. It is evident that for PG23 the phase transition temperature is higher than for PG160. The increase of the phase transition temperature with decreasing of pore diameters is related to the size effect.

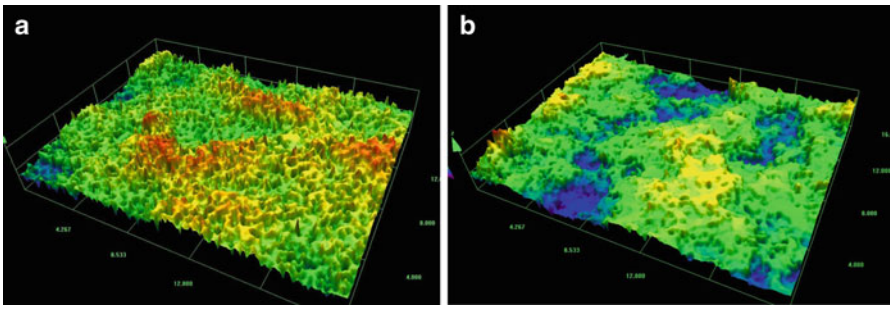

Fig. 16.1 Confocal graphs for PG160 (**a**) pure (**b**) with KNO_3 introduced from the melt

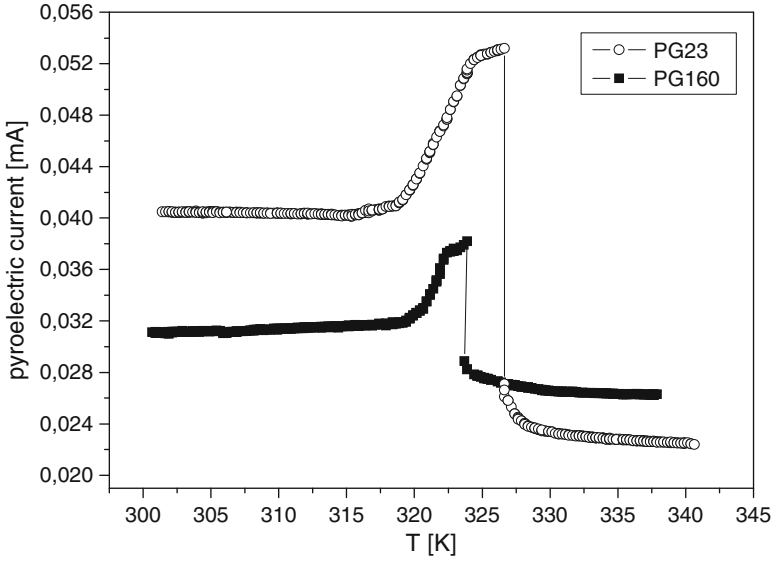

Fig. 16.2 Temperature dependence of the pyroelectric current for TGS embedded into PG 23 and PG 160 glasses

The phase transition temperature depends on the particle size according to the equation [8]:

$$T_c = T_\infty - \frac{6D}{\delta A d}, \tag{16.1}$$

where δ is the extrapolation length defined as the theoretical distance from the surface where the polarization drops to zero. This equation can be used for particle dimensions and thin film thickness [9].

The phase transition temperature shift is also related to the pressure effect caused by strain impacts due to the difference in thermal expansion coefficients of the glass matrix and nano-crystals.

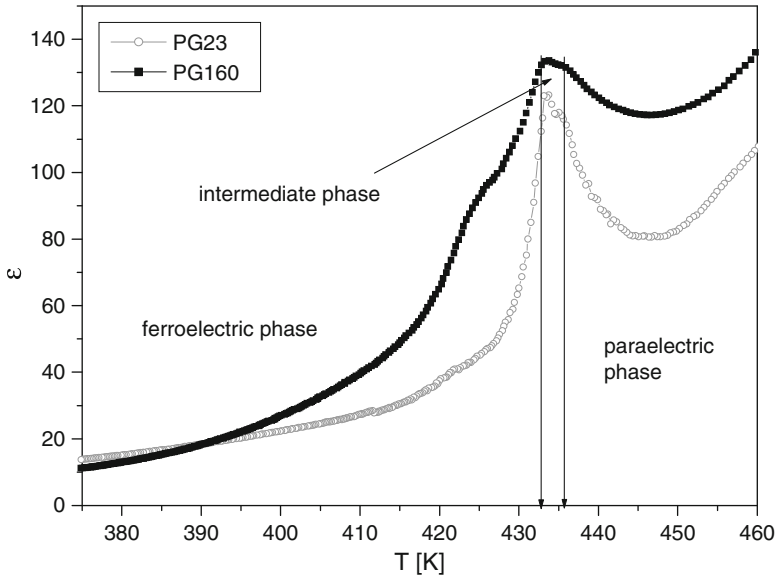

Fig. 16.3 Dependence of dielectric permittivity ε on the temperature for PG23 and PG160 filled by $NaNO_2$ introduced from a water solution for 1 kHz [7]

The phase transition in $NaNO_2$ introduced into porous glasses has been investigated by the dielectric spectroscopy. In Fig. 16.3 the temperature dependence of the dielectric permittivity ε for porous glasses filled by $NaNO_2$ from a water solution is shown. $NaNO_2$ crystals show the ferroelectric phase transition of order-disorder type at 436 K.

The transition passes through the intermediate phase is considered as an antiferroelectric or modulated phase. The appearance of the splitting of the maximum of the temperature dependence of the dielectric permittivity is related to the existence of the modulated phase in $NaNO_2$ confined in porous glass. It is worth noticing that this splitting in $NaNO_2$ nano-crystals has been shown for the first time. The existence of the antiferroelectric phase has been confirmed by the results of the calorimetric measurements [10].

The structure of $NaNO_2$ embedded into porous matrices has been determined from the diffraction neutron patterns [11]. The "diffraction" cluster size is much larger than the pore diameter. It is possible to state that nano- material can form a kind of "dendrite" clusters.

Physical properties of $NaNO_3$ nano-composites in a wide temperature range including the melt and phase transition temperature region have been investigated by the calorimetric method. $NaNO_3$ crystals show the second order phase transition of the order–disorder type at 549 K between two different symmetries of the trigonal system.

DSC thermograms obtained for $NaNO_3$ bulk crystal as well as PG23 and PG160 porous glasses embedded with $NaNO_3$ on heating and on cooling in the melting

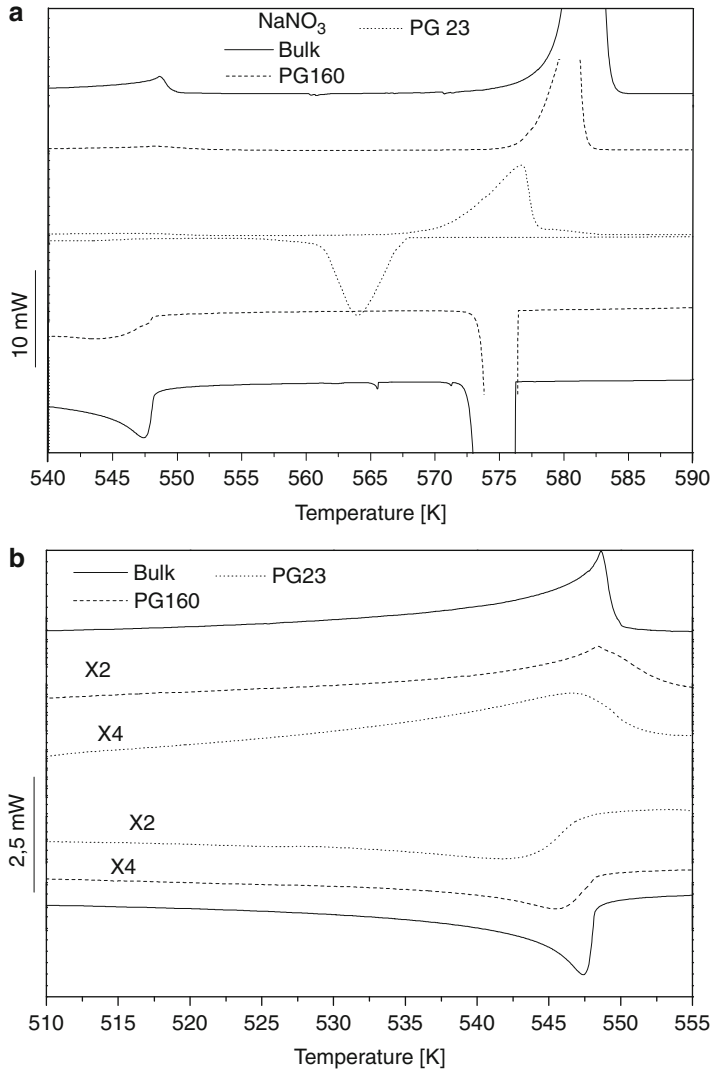

Fig. 16.4 DSC thermograms of $NaNO_3$ bulk crystals (B) as well as for PG23 and PG160 filled by the $NaNO_3$ obtained on heating and on cooling and in (**a**) a wide temperature range, (**b**) the structural phase transition temperature region [10]

temperature region is presented in Fig. 16.4a. The melting temperature of $NaNO_3$ crystal is higher than the melting temperature of $NaNO_3$ confined in porous glasses. This phenomena observed for glasses with different pore dimensions (2.5–10 nm) by Mu [12] can be explained as a formation of a new surface phase connected with the interaction between material introduced into pores and pores surface.

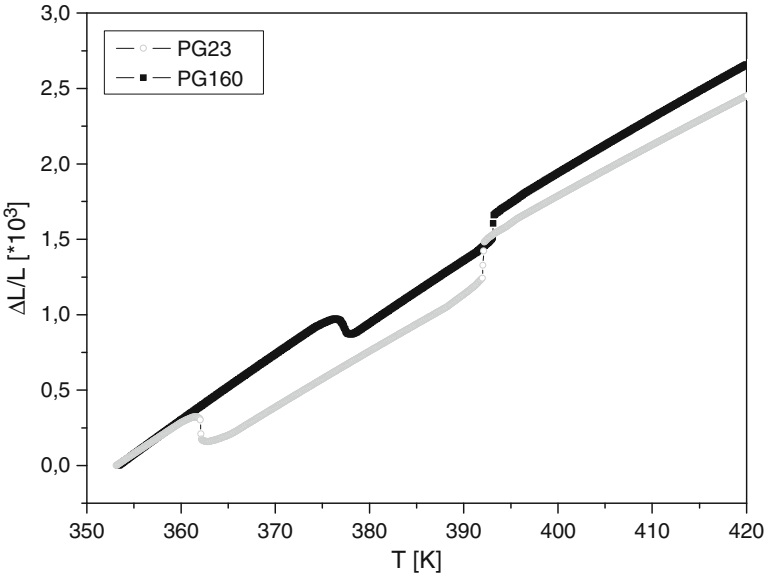

Fig. 16.5 The relative deformation dependence on the temperature of PG23 and PG160 glasses filled by KNO_3 introduced from the melt [13]

The results of the calorimetric measurements of $NaNO_3$ impregnated with PG23 and PG160 porous glasses and $NaNO_3$ crystal obtained on heating and on cooling near the phase transition temperature are presented in Fig. 16.4b. The specific heat anomaly small shift to lower temperatures with the decreasing pore dimensions for $NaNO_3$ introduced into porous matrices is observed.

This shift is related to the structural phase transition. The anomaly of the specific heat in $NaNO_3$ confined in porous glasses occurs in a wide temperature range i.e. a disordering process in the nanomaterial starts a temperature below the phase transition temperature. Mu has not observed the anomaly of the specific heat related to the phase transition in $NaNO_3$ nano-composites. The phase transition in nano-$NaNO_3$ has been observed for the first time.

The bulk KNO_3 crystal is very interesting material because ferroelectric phase is observed only when cooling at atmospheric pressure in the temperature range from 398 to 383 K.

The thermal deformation dependence on the temperature of porous glasses PG23 and PG160 embedded with KNO_3 from the melt during the cooling process is presented in Fig. 16.5. The data show that the phase transitions temperatures in KNO_3 introduced into porous glasses weakly depend on pore dimensions. The first order phase transition temperature from the paraelectric I into the ferroelectric phase III for PG23 and PG160 embedded with KNO_3 is lower than that for the bulk crystal (the change of the relative thermal deformation is observed at 391 K in both types of porous glasses).

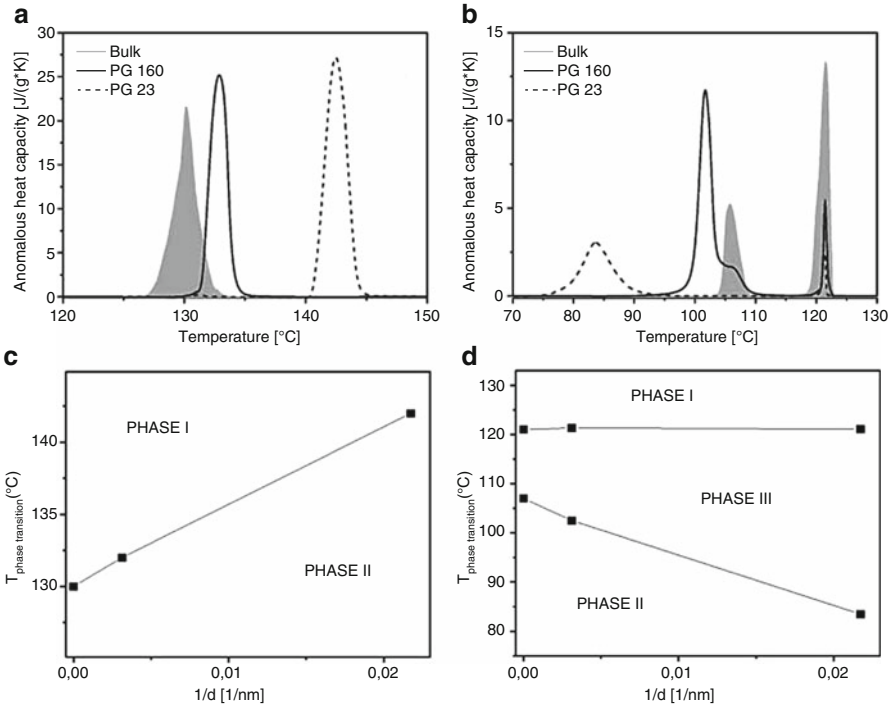

Fig. 16.6 The excess heat capacity dependence on the temperature for KNO_3 – bulk crystal, KNO_3 confined in PG160 and PG23 with (**a**) increasing temperature (**b**) decreasing temperature. The phase diagrams for the phase II-I transition is shown in (**c**), the I-III and III-II transitions in (**d**) [14]

The temperature connected with the phase transition from the ferroelectric phase III to the low temperature phase II in KNO_3 nano-composites is significantly lower than that in the bulk and it equals to 365 and 377 K for KNO_3 filled by PG23 and PG160, respectively.

The existence of the ferroelectric phase was confirmed by the calorimetric measurements performed during the cooling process (Fig. 16.6b). The peaks of the heat capacity appear near the expected (from the dilatometric measurements) phase transition temperatures. The data obtained for the heating process show that direct transition from the low temperature phase II to the paraelectric phase I (Fig. 16.6a) exists.

The dependence of phase transition temperature on reverse mean value of pore dimensions (the phase diagrams) for KNO_3 introduced into the porous glasses obtained from the calorimetric investigations for cooling and heating process are presented in Fig. 16.6c, d, respectively. The lowering tendency of the phase transitions is well visible.

MH_2PO_4 (where M = K, NH_4) crystals and their deuterium equivalents are a family of materials which are intensely studied and well known. A phase transition from the ferroelectric to paraelectric phase was observed at 123 K for

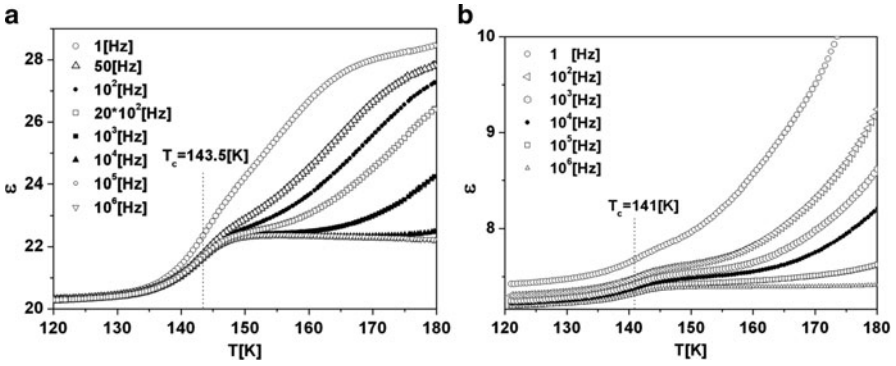

Fig. 16.7 Temperature dependence of the real part of the electrical permittivity for ADP introduced into (**a**) PG160 and (**b**) PG 23 porous glasses for different frequencies

KH_2PO_4 (KDP) crystals, whereas a transition to the super-ionic phase was observed at 450 K [15]. $PrNH_4H_2PO_4$ (ADP) crystal is the only one material which belongs to MH_2PO_4 family and shows anti-ferroelectric properties. The first-order phase transition to the anti-ferroelectric phase (the transition type: order-disorder) occurs at about 148 K for ADP crystals. It is worth noting that most of very interesting properties are connected with the proton ordering change in hydrogen bonds. At high temperatures KDP crystals show very high ionic conductivity (at the level of that for liquid electrolytes) [16, 17].

The dielectric permittivity dependence on the temperature in a wide frequency range for ADP embedded into porous glasses PG160, PG23 are presented in Fig. 16.7. It is evident that above the phase transition temperature the dielectric permittivity depends on frequency for both PG23 and PG160 glasses filled by ADP. For ADP embedded into porous glass PG23 additionally the low frequency dispersion is observed. It is worth to notice that the dispersion has not been observed either in bulk ADP or in porous glasses. A rapid increase of the dielectric permittivity above the phase transition temperature can be related to the ionic current. The increase of the dielectric permittivity is also observed for porous glasses embedded with KDP by Colla et al. [18].

The phase transition temperatures (estimated from the he $d\varepsilon'/dt$ curves for 1 kHz frequency) for ADP embedded into porous glasses are lower than those obtained for the bulk crystals and they are equal to 143.5 and 141 K for PG 23 and PG160, respectively [19].

In Fig. 16.8 the temperature dependence of the electrical conductivity of KDP embedded into porous glasses is presented.

The electrical conductivity has an activation character. The calculated values of the activation energies are equal to 0.55 and 0.60 eV for KDP confined in PG23 and PG160, respectively. They are lower than the activation energies in the bulk KDP crystal. It can be stated that the conductivity observed in confined KDP is connected with the proton motion.

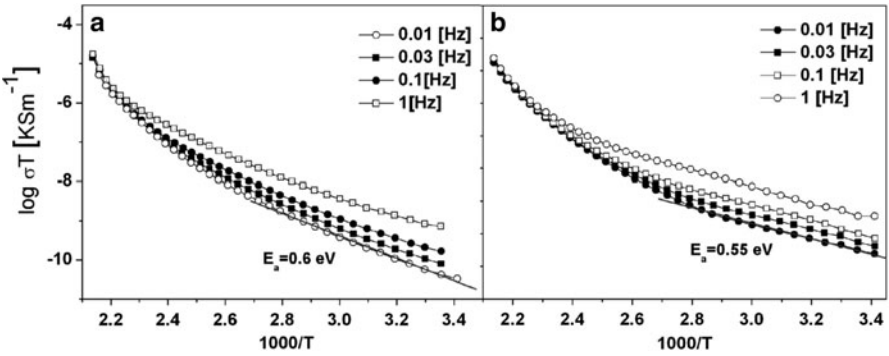

Fig. 16.8 log(σT) dependence versus 1000/T for KDP embedded into PG160 (**a**) and PG23 (**b**) for several selected low frequencies [20]

16.4 Conclusion

The results of electric and thermal measurements show that the observed sequence of phase transitions in ferroelectric microcrystals embedded into the porous glasses is similar to that in bulk crystals.

It has been shown that pore dimensions influence the phase transition temperature for the ferroelectric materials introduced into porous glasses. The negative size effect (the observed phase transition temperatures tend to decrease with the decreasing pore sizes) has been observed in porous glass filled with $NaNO_2$, $NaNO_3$, ADP, KDP and the positive one with TGS. The experimentally observed shift of phase transition temperatures is the superposition of the size effect and pressure effect created by the difference of thermal expansion coefficients of ferroelectrics nanoparticles and glass matrix.

References

1. Scott JF (2002) Ferroelectrics memories. Springer, Berlin/Heidelberg/New York
2. Beskrovny A, Golosovsky I, Fokin A, Kumzerov Yu, Kurbakov A, Naberezhnov A, Vakhrushev S (2002) Structure evolution and formation of a pre-melted state in $NaNO_2$ confined within porous glass. Appl Phys A 74:S1001–S1003
3. Tien Ch, Charnaya EV, Lee MK, Baryshnikov SV, Sun SY, Michel D, Böhlmann W (2005) Coexistence of melted and ferroelectric states in sodium nitrite within mesoporous sieves. Phys Rev B 72. doi:104105-1-104105-6
4. Jang EK, Woo JW, Yu I (1995) Rochelle salt nanocrystals embedded in porous glass. Application of Ferroelectrics, 1994.ISAF'94. Proceedings of the Ninth IEE International Symposium. CH34 16-50-7803-1847-1/95/1995IEEE:210–213
5. Balabinskaya AS, Ivanova EN, Ivanova MS, Kumzerov Yu A, Pan'kova SV, Poborchii VV, Romanov SG, Solovyev VG, Khanin SD (2005) Investigation into the electrical and optical properties of sodium nitrite and sodium nitrate nanoparticles in regular porous matrices. Glass Phys Chem 31:330–336

6. Rysiakiewicz-Pasek E, Lukaszewski P, Bogdanska J (2000) Investigation of correlation between mechanical properties and structure of porous glasses. Opt Appl XXX:173
7. Rysiakiewicz-Pasek E, Poprawski R, Polanska J, Urbanowicz A, Sieradzki A (2006) Properties of porous glasses with embedded ferroelectric materials. J Non-Cryst Solids 352:4309–4314
8. Zhong WL, Wang YG, Zhang PL, Qu BD (1994) Phenomenological study of the size effect on phase transitions in ferroelectric particles. Phys Rev B 50:698
9. Strukov BA, Davitadze ST, Shulman SG, Goltzman BV, Lemanov VV (2004) Ferroelectrics 301:157
10. Rysiakiewicz-Pasek E, Komar J, Ciżman A, Poprawski R (2010) Calorimetric investigations of $NaNO_3$ and $NaNO_2$ embedded into porous glasses. J Non-Cryst Solids 356:661–663
11. Beskrovny AI, Vasilovskii SG, Vakhrushev SB, Kurdyukov DA, Zvorykina OI, Naberezhnov AA, Okuneva NM, Tovar M, Rysiakiewicz-Pasek E, Jaguś P (2010) Temperature dependences of the order parameter for sodium nitrite embedded into porous glasses and opals. Phys Solid State 52(5):1092–1097
12. Mu R, Jin F, Morgan SH, Henderson DO, Silberman E (1994) The possible crossover effects of $NaNO_3$ confined in porous media: from bulk to clusters. J Chem Phys 100:7749
13. Poprawski R, Rysiakiewicz-Pasek E, Sieradzki A, Ciżman A, Polańska J (2007) Ferroelectric phase transitions in KNO3 embedded into porous glasses. J Non-Cryst Solids 353:4457–4461
14. Sieradzki A, Komar J, Rysiakiewicz-Pasek E, Ciżman A, Poprawski R (2010) Calorimetric investigations of phase transitions in KNO_3 embedded into porous glasses. Ferroelectrics 402 (1):60–65
15. Landoldt HH, Börnstein R (1982) Group III crystal and solid state physics. Springer, Berlin/ Heidelberg/New York
16. Chandra S, Kumar A (1990) Proton conduction in some solid hydrates and KDP-ferroelectric family materials. Solid State Ion 40:863
17. Diosa JE, Vargas RA, Albinsson L (2004) Dielectric relaxation of KH_2PO_4 above room temperature. Phys Status Solidi (b) 241:1369
18. Colla EV, Fokin AV, Kumzerov Yu A (1997) Ferroelectrcs properties of nanosize KDP particles. Solid State Commun 103(2):127–130
19. Marciniszyn T, Poprawski R, Komar J, Sieradzki A (2010) Phase transition in $NH_4H_2PO_4$-porous glass composites. Phase Transit 83(10–11):909–916
20. Sieradzki A, Ciżman A, Poprawski R, Marciniszyn T, Rysiakiewicz-Pasek E (2011) Electrical conductivity and phase transitions in KDP- and ADP-porous glass nanocomposites. J Adv Dielectr 1:337–343